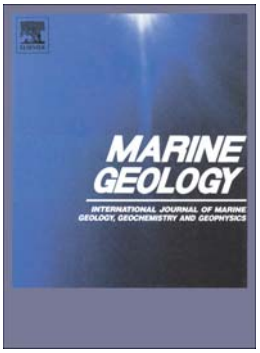

Wave breaking patterns control rip current flow regimes and surfzone retention

Sebastian Pitman, Shari L. Gallop, Ivan D. Haigh, Gerd Masselink, Roshanka Ranasinghe

PII: S0025-3227(16)30282-1
DOI: doi: 10.1016/j.margeo.2016.10.016
Reference: MARGO 5534

To appear in: *Marine Geology*

Received date: 31 May 2016
Revised date: 22 October 2016
Accepted date: 28 October 2016

Please cite this article as: Pitman, Sebastian, Gallop, Shari L., Haigh, Ivan D., Masselink, Gerd, Ranasinghe, Roshanka, Wave breaking patterns control rip current flow regimes and surfzone retention, *Marine Geology* (2016), doi: 10.1016/j.margeo.2016.10.016

Title:

Wave breaking patterns control rip current flow regimes and surfzone retention

Authors:

Sebastian Pitman[a*], Shari L. Gallop[b,a], Ivan D. Haigh[a], Gerd Masselink[c], Roshanka Ranasinghe[d]

Affiliations:

a. Ocean and Earth Science, National Oceanography Centre, University of Southampton, U.K.
b. Department of Environmental Sciences, Macquarie University, Australia.
c. School of Marine Science and Engineering, Plymouth University, U.K.
d. UNESCO-IHE and Deltares, Delft, The Netherlands; and University of Queensland, Australia

*Corresponding author: sjp1e13@soton.ac.uk

Abstract:

Recent research into rip currents has revealed the existence of multiple circulation patterns, meaning that no single escape strategy is appropriate in all situations. Rip circulation is influenced by surfzone morphology, which can be inferred from wave breaking patterns in video imagery. Wave breaking often occurs over the bars adjacent to the rip channel, with little breaking over the seaward end of the rip. However, under varying wave and tide conditions, breaking can also occur at the seaward extent of rip channels. Here, we use this difference as a novel wave dissipation parameter to classify a rip channel as either 'open' or 'closed' in terms of rip-head wave breaking. A 4-day field study provided Lagrangian rip current data at a macrotidal, dissipative beach monitored by a coastal imaging system. Using this new parameter, rip channels that were identified as closed exhibited a 31 % increase in current speeds and 43 % increase in horizontal vorticity compared to open channels. The transition between open and closed channels occurred over a single tidal cycle, which altered surfzone retention rates. Closed channels promoted surfzone retention, with < 25 % of drifters exiting the surfzone. In comparison, open channels were more conducive to exchange, with exit rates up to 91 %. Analysis of the Royal National Lifeboat Institution lifeguard rip incident database showed that open rips were disproportionately represented in the occurrence of rescue events, and calculated here to be twice as dangerous as closed rips. The use of this new open/closed parameter could be used by surf lifesaving organisations, and may have implications for the cross-shore exchange of sediment and pollutants.

Keywords:

Video imagery, beach state, rip current, beach rescue, wave breaking, Perranporth

1. Introduction

Rip currents (rips) are hazardous offshore flows in the surfzone of beaches worldwide, with typical velocities of 0.5 – 0.8 m s^{-1}, and can exceptionally reach 2 m s^{-1} (MacMahan et al., 2006). Rips are seen as key drivers of cross-shore shore sediment transport (Aagard et al., 1997), and have been observed to move significant amounts of sediment offshore to the inner continental shelf (Cook, 1970), with obvious implications for storm erosion and post storm recovery.

Unsuspecting bathers can be transported offshore in these narrow, fast currents, and often require rescue. Consequently, rips present a global problem for recreational beach use; in the U.K., 68 % of incidents on beaches patrolled by the Royal National Lifeboat Institution (RNLI) are attributed to rips (Scott et al., 2008). In Australia, rips were a factor in 44 % of recorded beach drownings over a seven-year period (Brighton et al., 2013). Recent research has focussed on assessing the effectiveness of various escape strategies for people caught in rips (Miloshis and Stephenson, 2011; McCarroll et al., 2014a, 2015; Castelle et al., 2015; Van Leeuwen et al., 2015). The traditional promoted strategy was (and still is in many places) to swim parallel to the shore (Castelle et al., 2015). This advice is based on the assumption of a 'typical' rip, where the current is directed offshore perpendicular to the shore, and exits the surfzone into deeper water (Shepard et al., 1941), herein referred to as *rip exits*. However, Lagrangian measurement of rips over the last decade (Austin et al, 2009, 2010, 2014; MacMahan et al., 2010; McCarroll et al., 2014b; Scott et al., 2014) have shown that there is a wide variety of rip circulation patterns, including circulatory, and angular flow (i.e., not perpendicular to shore). Under such flows, the 'swim-parallel' strategy may not be appropriate and could even reduce chances of escape (Castelle et al., 2015). The current circulation pattern is therefore of paramount importance when considering the risk posed by rips and the formulation of beach safety advice.

Rip activation (the establishment of a depth-uniform offshore-directed flow) has been attributed largely to alongshore gradients in the radiation stresses of breaking waves (Longuet-Higgins, 1970), and variations in nearshore bathymetry that induces spatially variable patterns of wave breaking (Bowen, 1969). The requirement for wave breaking on offshore bars is widely accepted as a pre-requisite for topographic rip activation, with increasing intensities of wave breaking creating stronger rip circulations (Sonu, 1972; Dalrymple, 1975; Wright et al., 1979; Aagard et al., 1997; MacMahan et al., 2006). Rip flow is also tidally-modulated, with water level controlling the degree to which waves interact with bathymetry. This interaction transforms wave breaking patterns and varies flow constriction through channels over the tidal cycle (Austin et al., 2010). Maximum rip speeds are generally observed around low tide, when the interaction of breaking waves with the morphology is greatest (Aagaard et al., 1997; Brander, 1999; Austin et al., 2010, 2014; McCarroll et al., 2014b; Scott et al., 2014). In macrotidal environments, higher tidal levels can switch off rip circulation entirely as a result of the cessation of wave breaking over the bar (Austin et al., 2014).

The combination of these controls on nearshore circulation create one of two responses in an active rip: 1) rip exit, or 2) recirculation within the surfzone. Previously, the effect of wave breaking patterns on circulation has been opportunistically and qualitatively discussed as a result of field measurement (Scott et al, 2014). However, no quantitative link between breaking patterns and circulation type has been investigated. Therefore, here we hypothesise that an important control on this circulation is whether the rip exhibits an ‘open’ connection to the region offshore of the surfzone (hereafter referred to as the offshore) in terms of wave breaking, or whether wave breaking acts to ‘close’ the rip channel. A rip channel that is ‘closed’ in terms of wave dissipation (i.e., waves are breaking at the seaward edge of the rip, across the rip channel and/or on the rip head bar) may be more likely to exhibit circulatory

behaviour, as a result of wave setup in the region of breaking. Conversely, a rip channel that is 'open' to the offshore region (i.e., no wave breaking at the seaward edge) may be unhindered by wave breaking processes, and therefore the current may exit the surfzone.

Observational changes in wave breaking have been documented by various researchers; Brander (1999) provided a conceptual model of rip activity based on the Wright and Short (1984) beach state model, and discussed changes in morphology that are inferred from changes in the breaking pattern. Brander (1999) describes downstate change in morphology as a result of decreasing wave conditions, and the associated changes in rip channel configuration. The shift in channel configurations is accompanied by different patterns of wave breaking over the reconfigured bar system. Of particular interest was the longshore bar-trough state proposed, which is akin to an open rip, and the transverse bar rip which exhibits a welded rip head bar, akin to a closed rip described above. Whereas Brander (1999) showed virtual state transitions as a result of wave conditions, the work of Austin et al. (2010) took a similar approach with tidal control. They highlight how lowered water levels produce behaviourally similar results to that of a wide-spread accretion (down-state transition) in the beach state model, maximising bar relief. Quartel (2009) later attempted to classify intertidal rip channels as either open or filled, in terms of sedimentation, rather than wave breaking patterns, which is the focus of the current contribution. Both types were defined as funnel-shaped, where open rip channels showed a shoreward narrow end, with a clear opening through the wave break point to deeper water, similar to the definition of open used here. In contrast, a filled rip channel was an inverse-funnel (wider end towards the shore). A filled rip is said to develop as a result of sediment infilling, whereas a closed channel in terms of wave breaking is the result of lower water levels inducing wave breaking at the offshore extent of a rip channel. Channels were classified from low tide video images, using the visual contrast between dry sand and water or wet sand.

While Brander's (1999) model and the work of Quartel (2009) discussed variability over timescales of *O*(days-weeks), the control exerted by tidal modulation of wave breaking can produce similar transitions over a single tidal cycle (Austin et al., 2014), whereby low tide levels can mimic a down-state transition in beach state. Quantifying these wave breaking patterns using *in situ* measurements is difficult. However, such patterns can be relatively easily identified using coastal imaging systems, such as Argus (Holman and Stanley, 2007), Cam-Era (Gallop et al., 2011; Blossier et al., 2016), and WavePack (Gal et al., 2014). These cameras typically take high frequency, half-hourly images of the beach and nearshore during daylight hours (Holman and Stanley, 2007). Time exposure (timex) images are the most commonly used output, representing the time-mean of all frames over a sample period, typically 600 images collected at 1 Hz (Guedes et al., 2011). Timex images can reveal persistent processes, such as wave breaking over submerged sand bars (Lippmann and Holman, 1989), which appear as distinct, high-intensity white bands (Lippmann and Holman, 1989, 1990; Plant and Holman, 1998; Kingston et al., 2000); while deeper areas, such as rip channels between sand bars, appear as darker areas (Ranasinghe et al., 1999, 2004; Holman et al., 2006).

Many studies have measured rips *in situ* (Austin et al, 2009, 2010, 2014; MacMahan et al., 2010; McCarroll et al., 2014b; Scott et al., 2014), and using video imagery (Ranasinghe et al., 1999; Bogle et al., 2001; Whyte et al., 2005; Holman et al., 2006; Turner et al., 2007; Gallop et al., 2009, 2011), but very little research has attempted to combine in situ measurement of rips with video images for quantitative means. One study addressing this previously was Austin et al. (2010), which quantified wave roller dissipation over the sand bar at Perranporth, U.K., and linked the intensity of breaking to rip pulsations. They determined how changes in the intensity of wave dissipation activated the rip, but not how patterns of dissipation influenced circulation pattern, i.e., if a rip is retained within, or exits the surfzone.

A possible link between readily observable phenomena, such as wave breaking, and the danger level of prevailing rip currents could have practical benefits. For instance, an indication of whether rip currents are likely to be retained within, or exit, the surfzone based purely on real time video imagery could be very useful to beach safety practitioners, who may elect to increase coverage or patrols on days where rips appear more dangerous in imagery.

The overall aim of the present study is to gain new insights regarding the influence of wave breaking patterns on rip current circulation and therefore the hazard presented to beach users. In this contribution we define a new parameter to classify wave breaking patterns around rip currents. The aim was addressed through two objectives. The primary objective is to quantify the influence of open and closed rips on surfzone exit rate and the second objective is to determine the influence of wave breaking patterns on rip rescue events. To this end, we use an exemplar of an exposed macrotidal, low tide bar/rip beach in southwest England. Data were collected from a single north Cornish beach but are transferable to other exposed sandy beaches with large tidal ranges and low-tide rip morphologies.

2. Field site

Perranporth beach (Figure 1) is a 3.5-km long beach comprised of medium ($D_{50} \approx 0.3$ mm) sand (Austin et al., 2014). Perranporth is a popular swimming and surf beach, and holiday destination. The beach is patrolled by the RNLI during summer, and some public holiday weekends throughout the year. The beach has a wide (500 m) intertidal area at the southern end, which narrows into a 250 m wide intertidal area to the north. The mean spring tidal range is ~ 6.3 m (macrotidal) (Austin et al., 2014). The beach faces west-north-west towards

the Atlantic and is subject to medium energy conditions with mean offshore significant wave height (H_s) of 1.5 m, maximum wave heights (H_m) of 2.4 m, and peak periods (T_p) of 10.5 s. Research on surfzone currents at Perranporth is well established, through a number of field deployments (Austin et al., 2009, 2010, 2013, 2014; Scott et al., 2014).

3. Data & Methods:

3.1 Field conditions

A field experiment was conducted at Perranporth from 16 to 19 May 2014, coinciding with spring tide, where the range was 6.4 m. Sea-level data from the Port Isaac tide gauge (36 km north east of Perranporth) was obtained from the Channel Coastal Observatory (CCO) online repository (www.channelcoast.org) (Figure 2a). Wind and wave data were also obtained from the CCO, with waves measured using a directional wave rider buoy approximately 1 km offshore of Perranporth. The hydrodynamic conditions during the study were typical of Perranporth and during the deployments, H_s reached 1.5 m on the final day, with lower energy conditions (0.5 m < H_s < 1.25 m) during the other days (Figure 2b). Maximum T_p coincided with the highest waves on the final day, with fluctuations between 8 and 12.5 s over the 4-day data collection period (Figure 2c). The incident wave field propagated approximately shore-normal throughout (Figure 2d). Wind was onshore over the first three days, with a low wind speed (U = 2.5 m s $^{-1}$) on the first two days and high larger wind speeds (U = 8.8 m s $^{-1}$) on third day. On the final day of the experiment, a weak ($U \approx$ 1 m s $^{-1}$) offshore wind prevailed (Figure 2e - f). The beach exhibited a typically double bar state (Masselink et al., 2014) with the inshore and outer bars at c. 500 and 800 m offshore of the mean high water springs shoreline, respectively (Figure 3).

3.2 Bathymetry and topography

The bathymetry was measured on 17 May 2014 using an Inflatable Rescue Boat (IRB), fitted with a single-beam echosounder. Bathymetry was collected in cross-shore profiles spaced 25 m apart over the nearshore bar, and 50 m offshore of the outer bar. Subaerial beach topography was measured using an All-Terrain Vehicle (ATV) fitted with RTK-GPS, in alongshore lines spaced 10 m apart. The subaerial topography and submerged bathymetry were merged with significant overlap for quality control (Figure 3a). The bathymetry presented here is the residual morphology (Figure 3b), following the approach of Austin et al. (2010). The residual bathymetry is obtained by subtracting the cross-shore linear trend surface over the entire intertidal area from the measured bathymetry at that same cross-shore transect. This residual value acts to highlight the positive and negative relief from the linear profile, which allows appreciation of the nearshore features with which the incident wave field interact.

3.3 Video imagery

Perranporth is monitored by a set of three Argus cameras located on Droskyn Point at the southern extreme of the beach (Figure 1), 48 m above mean sea level (Huntley et al., 2009). The first two cameras were installed in 1996, with the third installed in 2010 (Scott et al., 2014). This study uses half-hourly, geo-rectified 10-minute time exposure (timex) images (Figure 3c) in the local Argus co-ordinate system. In general, there is potential that the imagery at this frequency aliases the wave group frequency, which has before been postulated as an important process in controlling rip current velocity pulses (Shepard et al., 1941; Sonu, 1972; Aagard et al., 1997). However, Scott et al. (2014) estimate wave group frequency at Perranporth to be between 25 – 250 secs, and the chosen image sampling frequency of 600

secs ensures that at least one wave group is captured per timex image. Furthermore, the nature of the timex image ensures that the maximum extent of wave breaking is captured, and therefore aliasing effects do not present a significant problem for later analysis. Timex images for tidal levels less than 3m CD from 2009 – 2013 were classified using the segmentation method developed by Pitman et al. (2016) into 'open' or 'closed' rips (Figure 4). This classification involves thresholding images (Figure 4a – b) based on greyscale intensities into a binary image, where white values show wave breaking and black pixels show deeper channels (Figure 4c – d). The binary image allows for a simple, objective visual classification of either 'open' or 'closed' channels. A threshold from 0 to 1 is selected in order to produce the black and white pixels required for the binary image (Figure 5). The threshold (τ) used here was 0.5, and sensitivity analysis showed that for $0.3 < \tau < 0.7$, the technique was robust, with 95 % of images being classified correctly by all values of τ within this range (Figure 5). It is unfortunate that the Argus camera was unserviceable for the period 20 – 23 Jul and also 6 – 22 Aug, when most incidents occurred. However, investigation of the images captured immediately prior to and following these outages showed the presence of numerous and prominent open rip channels. Furthermore, the wave conditions between 23 Jul and 23 Aug were low energy (mean H_s = 1.02 m), with no storms and therefore it is likely that the prominent open rip channels persisted throughout the period.

3.4 Lagrangian drifters

Lagrangian flow measurements were recorded using six surfzone GPS drifters. The drifters were modified from the Schmidt et al. (2003) design, and were similar in construction to those used in recent field studies (MacMahan et al., 2009; Austin et al., 2012; Scott et al.,

2014, 2016). The OEMStar low cost single frequency GNSS receiver was used to collect raw L1 GPS carrier phase signals, which were logged on an Antilog serial data logger. The raw signal was post processed using the RTKLIB programme, against data from a static Trimble base station located on Droskyn Point (Figure 1), reducing the positional error to < 0.3 m. MacMahan et al. (2009) demonstrated the method to be appropriate to resolve flows on the order of 0.05 m s^{-1}.

A total of 195 deployments were made over the four days, during 4-hour periods centred on low tide (Figure 2). Drifters were predominantly deployed individually by field assistants into the rip channel and feeder areas, in water depths of up to 1 m; with entry times recorded by an observer on the beach. Drifters were also deployed on sand bars either side of the main channel in order to maximise coverage of the entire circulatory system. Occasionally, water depth hindered these deployments, and subsequently some drifters were deployed by the IRB seaward of the bars. Drifters were retrieved (by assistants or IRB) when they entered water too shallow to allow free-floating, or when they washed along- or off-shore to such an extent that it exited the study area or entered the area preferentially marked by the RNLI for bathing. Retrieved drifters were immediately redeployed.

Each individual deployment was classified visually into one of four categories: 1) linear exit; 2) circulation then exit; 3) circulation with no exit; or 4) 'other'. These classifications are similar to those used in other studies (MacMahan et al., 2010; Austin et al., 2013; Scott et al., 2014; Gallop et al., 2015; 2016a). A linear exit was defined as the drifter moving offshore immediately from the time of deployment, to beyond the edge of the surfzone. 'Circulation then exit' was when drifters had a significant portion of onshore movement before moving offshore, or when the drifter made at least one complete re-circulation before moving offshore beyond the edge of the surfzone. 'Circulation with no exit' was defined as movement fully contained within the surfzone. Under this condition drifters would typically

rotate 3 or 4 times over periods *O*(15 mins) before washing alongshore or onshore. In an extreme case, one drifter recirculated 13 times over 80 mins before washing alongshore. 'Other' was defined as occasions when the drifter washed ashore, or travelled significantly alongshore within the surfzone, without circulation in or around the rip channel.

The spatial domain in which the drifters circulated was divided into 10 x 10 m cells (Figure 3d and e) and all drifter data for subsequent discrete time periods were calculated within these cells. This cell size is appropriate to quantify the circulation pattern, given that typical scales of rip circulation are *O*(100 m), and is comparable to previous studies (MacMahan et al., 2010; McCarroll et al., 2014b). All GPS observations were binned into 10 s windows and averaged into one location observation per window, resulting in observations at a frequency of 0.1 Hz. Following the work of Spydell et al. (2007) and MacMahan et al. (2010), observations in the same grid square were grouped into one independent observation. If the drifter later re-entered the grid square, it would be considered a new independent observation if it had travelled a significant distance (defined as the length of the grid square) before doing so. A re-entering drifter was independent when $t>l_g/U$ (MacMahan et al., 2010), where t is elapsed time, l_g is the grid square size and U is the average drifter speed whilst in transit outside of the gridsquare. Velocity and direction measurements were then calculated for bins with at least 5 independent observations, following Spydell et al. (2007) and MacMahan et al. (2010). Velocity calculations (Figure 3e) were based on the mean of independent observations in each grid square ($\bar{U}'$). Following McCarroll et al. (2014b), the overbar is herein used as a denotation for a value based on a grid square mean, and the prime symbol denotes the use of independent observations. The 10 s window was used because the maximum drifter speeds from previous Perranporth experiments (Austin et al., 2009; Scott et al., 2014) were typically around 1 m s^{-1}, equating to up to 10 m horizontal displacement over

the 0.1 Hz window. This is comparable to the 10 x 10 m cells that were used to construct the spatial domain for processing.

The circulation of rip currents is of paramount importance in this study and therefore we present a measure of vorticity (Γ) throughout (Figure 3f). Vorticity is defined as the change in orientation of a parcel of water, without change in area or shape (Molinari and Kirwan, 1975; MacMahan et al., 2010) and is a parameterisation of the local rotational motion of a fluid, or velocity shear (McCarroll et al., 2014b). Vorticity has been calculated using the weighted central difference method (MacMahan et al., 2010), as follows;

$$\Gamma = \frac{dv}{dx} - \frac{du}{dy} \quad (1)$$

where u and v are the vector components of $\bar{U}'$ at point x,y.

The majority of data were collected from one rip channel (x = 700 m, y = -400 m; Figure 3), with the number of independent observations (n) greater than 50 at 0.1 Hz recorded in the main channel (Figure 3d). The feeder and offshore regions also received good coverage, with n > 10 at 0.1 Hz. Drifters travelled alongshore as far as y = -900 m; however, typically n < 5, and thus the remainder of discussion in this paper is constrained to within the white box shown in Figure 3 (-200 m > x > -600 m; 900 m > y > 500 m).

3.5 Rip incident data

Rip incident data were supplied for Perranporth by the RNLI for 2009 – 2013. The RNLI record an incident every time they intervene. They record time and location, demographic data, qualitative observations of meteorological and hydrodynamic conditions and, crucially, information on the cause of the incident (e.g., inexperience, rip currents, tidal cut off, etc.). Of all recorded incidents at Perranporth, 250 (some of which were for multiple persons) were

attributed at least in part, to rip currents. During these incidents, there were 400 people rescued and assistance was offered to a further 215 people. The RNLI estimates that without intervention, 16 lives would have been lost over the 5-year period at Perranporth. For each incident, the rip channel was classified as open or closed from timex images (if images were available). Of the 250 incidents, 185 were used for image classification and 65 incidents were disregarded as a result of either fouled images or their occurrence at mid- to high-tide. Austin et al. (2014) showed that rips on Perranporth are inactive when water depths are above ~3 m, and thus, incidents during these periods have been omitted from further analysis. Of the remaining 185 images, 82 were classified as closed and 103 as open. A limitation of the RNLI dataset is that the exact location of rescues in relation to the surfzone morphology is not recorded. For each incident, the lifeguards report an approximate alongshore zone (generally 50 m-wide) of the incident relative to their primary position. Rip spacing at Perranporth is typically *O*(400m), which means the approximate rescue location supplied by the lifeguards is sufficient to estimate rescue location, in relation to a specific rip channel. The rip channel chosen for the field experiment is one of the most persistent topographic rip channels at Perranporth, present over a number of years in the imagery with a total alongshore oscillation over an area no greater than 400 m. The RNLI dedicated bathing area is generally located ~250 m alongshore from this prominent rip.

4. Results:

4.1. Wave dissipation and circulation

The first objective of this study is to quantify the influence of open and closed rips on surfzone exit rate. During the experiment, two dominant flow regimes were observed: 1) circulation confined within the surfzone; and 2) surfzone exits. On 16 May, the incident wave

field was near shore-normal, with weak ($U \approx 2.2$ m s^{-1}) onshore winds (Figure 2). The wave conditions were some of the most energetic observed during the study ($H_s \approx 1.25$ m, $T_p \approx 12$ s), but waves were still less steep than the summer average ($H_s \approx 1.1$ m, $T_p \approx 8.3$ s). Figure 6 shows the overall circulation patterns each day. Mean and max speeds were calculated over each 4-hour deployment. The combination of these factors drove a symmetric (MacMahan et al., 2010) rip, with the main channel extending perpendicular to the shore at y = 350 m (Figure 6a) and recirculations on either side of the rip neck in opposing gyres. The larger of the two cells is the clockwise circulation with the peak onshore return flow from this cell at y = 420 m. A counter-clockwise circulation is also observed, although the circulation cell is much weaker and less established. Mean offshore-directed flow through the centre of the channel was ≈ 0.8 m s^{-1} throughout the course of the day, with peak flows reaching ≈ 1.1 m s^{-1}. Mean onshore flows ranged from 1 m s^{-1} in the clockwise circulation to 0.5 m s^{-1} in the counter-clockwise flow (Figure 6a). These two circulation regimes existed in temporal isolation from each other (Figure 7a). Between the first deployment at 10:47 and 11:37 flows were predominantly confined to the counter-clockwise circulation cell, with recirculation dominating and few surfzone exits. Throughout the course of the day, the counter-clockwise circulation cell became less prominent as a clockwise circulation developed. Recirculations continued to dominate flow patterns until after 13:15 when surfzone exits became the primary form of flow pattern.

The clockwise circulation persisted into 17 May, with the counter-clockwise cell decaying into a purely offshore component (Figure 6b). Winds persisted in the onshore direction and increased in speed ($U \approx 3$ m s^{-1}), but wave conditions ($H_s \approx 0.75$ m, $T_p \approx 10$ s) were comparable to the previous day (Figure 2). Mean offshore rip flows were comparable to the previous day; however, there was a slight reduction in peak offshore flows to 1 m s^{-1}. Mean onshore flows reduced to around 0.7 m s^{-1}. Early afternoon showed, again, a split circulation

between both clockwise and counter-clockwise cells (Figure 7b); however, as the day progressed the counter-clockwise circulation ceased. This day was predominantly characterised by surfzone exits as the dominant flow regime.

Circulation on 18 May was dominated by an alongshore component to the flow. Strong onshore winds with an alongshore element dominated this day ($U \approx 8.5$ m s^{-1}), with wave conditions largely unchanged from the previous day ($H_s \approx 0.65$ m, $T_p \approx 9$ s). The rip was fed alongshore by the strong prevailing wind and wave direction, before sharply turning offshore through the rip neck (Figure 6c). Rather than a typical rip head dispersion, whereby the current disperses in all directions, there was a further strong change in direction alongshore, again in the direction of the prevailing wind and wave fields. This alongshore dispersion was only evident later in the day (Figure 7c), whereas drifters in the first deployment (12:25 – 13:10) exited the surfzone almost directly into the prevailing wind direction. Mean offshore flow speeds on this day were the lowest of the experiment, peaking around 0.4 m s^{-1}.

Circulation on 19 May was confined almost entirely within a well-established counter-clockwise cell (Figure 6d), aligned with the direction of a weak ($U \approx 2$ m s^{-1}) offshore wind (Figure 2). Wave conditions were most energetic during this period ($H_s \approx 1.5$ m, $T_p \approx 13$ s). Offshore current speeds throughout the day were consistently the highest observed during the experiment, often in excess of 1 m s^{-1} (Figure 7d).

The classification of rip channels as open or closed allows comparison with the observed drifter behaviour described above (Figure 8). In the closed scenarios (Figure 8a – d), there were 6 occurrences when drifters exited the surfzone, but the dominant circulatory regime was circulation with no exits (n = 55). There is a clear demarcation at the offshore extent of wave breaking that coincides with the offshore extent of the majority of drifter tracks during closed conditions. This subsample is comparable to the entire dataset, where there were 23

exits compared to 113 circulations (Figure 9), with no exits during conditions when wave breaking enclosed the rip channel (Figure 8). Of the 4 closed scenarios shown, Figure 8a had a high number of exits (24 %, n = 4) compared to the other periods when the channel was classified as closed. Three of these exits subsequently re-circulated back through the breaking waves after periods between 50 – 140 s. For most of the deployment, drifters were retained within the surfzone and only one drifter exited and did not return.

When considering the open rip scenarios (Figure 8e – h), there is a marked shift towards the dominance of surfzone exits or circulation resulting in an exit. Most of these exits occurred through the middle of the channel. Typically, drifters that flowed offshore in regions of wave breaking either side of the channel failed to exit the surfzone and instead recirculated onshore. In the closed rips, there was a consistent dominance of 'recirculation' in the drifter behaviour. Conversely it may be expected to see a dominance of 'exits' in the open channels; however, the opening of the channel appears only to increase the chance of an exit, rather than making surfzone exits the dominant form of circulation. For example, at times, despite the open channel, there were equal numbers of exits and recirculations (Figure 8f). Over the course of the experiment, the exit rate in open rip channels was 63 % (Figure 9), compared to 17 % in closed channels. Chi Squared analysis of the two channel conditions shows the difference in flow regimes to be statistically significant at 99.9 % confidence ($p < 0.001$).

The dominance of surfzone retention under closed conditions coincides with higher current speeds and increased vorticity (Figure 10) in closed rips. The average offshore-directed drifter velocity under closed conditions was 0.59 ± 0.15 m s^{-1} (Figure 10a), which is a 31 % increase over open conditions, where average speeds were 0.45 ± 0.17 m s^{-1} (Figure 10b). A two tailed t-test found the difference to be significant at 99.9 %. The higher values in closed rips ($\bar{U}' \approx 0.8$ m s^{-1}) were observed mid channel (Figure 10a), showing an increase in speed from the peripheral feeder zones to the rip channel itself. In open rips the lowest offshore-

directed velocities ($\bar{U}' \approx 0.3$ m s^{-1}) were located at the onshore extent of the channel (Figure 10b), with velocities doubling as the current extends to the edge of the surfzone. Despite this increase in velocity offshore, the mean speeds at the edge of the surfzone are still lower than the average mid channel speeds of a closed current. Vorticity was also maximum in the closed rips, with a mean absolute vorticity of 0.023, compared to 0.016 in open channels, showing a 43 % increase in absolute vorticity in closed channels. The standard deviations were large (± 0.017 and ± 0.014 respectively), but a t-test showed the two populations to be statistically different at 99.9%. A large band of strong ($\Gamma > 0.02$) anticlockwise circulation was evident in the feeder region (Figure 10c, x = 550 m, y = -350 m) of closed channels, whereas the coinciding region in open channels had a much more fragmented band of anticlockwise circulation, albeit of comparable magnitude. In the main channel, open conditions are characterised by minimal vorticity ($|\Gamma| < 0.005$), indicative of a linear, non-rotational offshore flow. Conversely, in closed channels there are large areas (*c.* 50 x 50 m) of strong clockwise rotation ($\Gamma < -0.02$) before the current reaches the edge of the surfzone. The effect of this rotation is to promote surfzone retention as drifters are deflected alongshore in the breaking waves.

The patterns of wave breaking showed the propensity to change between open and closed channel scenarios on short (hourly) timescales, as a result of tidal modulation over the morphological template. This was well demonstrated on 17th May 2014 which was initially dominated by an open rip (Figure 7b), and a high proportion of drifters exiting the surfzone and minimal recirculation (Figure 7b: 1200 - 1238 hrs). However, by low tide (Figure 7b: 12:38 – 13:16 hrs), there was a well-defined closed channel, coinciding with the flow pattern changing to nearshore circulation without exits. As the tide level increased, the expression of the morphology produced an open channel (Figure 7b: 13:16 – 14:32 hrs) and the number of exits increased.

4.2 Wave dissipation and swimmer safety

The second objective of this study is to determine the influence of wave breaking patterns on rip rescue events. RNLI rescue data for 2009 – 2013 showed 25 incidents when 5 or more people were rescued, or where the RNLI predicted there would have been loss of life without intervention. Here we classify these events as 'major' incidents. Of the 25 major incidents, 18 were analysed. Of the seven discarded, three high tide incidents were outside the scope of the study, two major incidents occurred > 1000 m from the lifeguards and an additional two incidents occurred during a time when the camera lens was fouled. Incidents predominantly occurred during British school summer holidays (Jul – Aug), with most incidents occurring between 23 Jul and 23 Aug 2013. In this time, there were 6 major incidents, with a total of 49 people rescued and 5 lives saved.

Open channel morphologies were observed in 78 % (14) of the major incidents, compared to 22 % (4) incidents occurring under closed channel configurations. Of these 14 'open rip' major incidents, the RNLI rescued 85 people and saved the lives of 10, in comparison to 32 rescues and 3 lives saved under closed conditions. This trend in major incidents is echoed in the incident record as a whole (Table 1), where there were a total of 169 (58 %) rescues from open rip channels during the 5 years, compared to 42 % from closed channels. Of all the lives saved, 77 % were from open channels. When considering incidents involving body boarders, 76 % of rescues occurred in open channels. Rescues involving swimmers have a similar trend, with 90 % (18 incidents) of swimmer rescues occurring in open channels. The RNLI cited inexperience as a factor in 35 incidents in open channels, compared to only 16 in closed channel scenarios (Table 1). An analysis of one lifeguarding season's worth of data (May – Sep 2013) showed that open rips occurred in 109 (40 %) of images, whereas closed rips

occurred in 163 (60 %) of images. Using this as an overall estimate of the prevalence of open and closed rip channels, the data can be normalised as per Equation 1:

$$\frac{{}^{B_o}/_{B_r}}{{}^{A_o}/_{A_r}} \quad (2)$$

where *B* and *A* represent closed and open rip channel conditions respectively, *o* is the occurrence of each condition and *r* is the number of rescues in each condition. Using Eq 1 it is possible to quantify that open rips are twice (2.08) as dangerous as closed rips. Here, no information was available on the number of beach users at each time, and therefore exposure to the hazard has been assumed to be uniform throughout.

5. Discussion:

The first objective of this research was to quantify the effect of open and closed rip channels on surfzone exit rate. A rip that is visually classified as closed is likely to exhibit recirculatory behaviour. Wave breaking around the channel closes the rip, which increases the vorticity and the current speed and results in the formation of a circulatory current which encourages surfzone retention. In open rips, the absence of wave breaking at the offshore extent of the rip channel decouples the offshore morphology from the rip channel circulatory system. A slower current then persists that extends offshore of the surfzone and increases the exit rate. Thus the likelihood of being ejected from the surfzone by an open rip channel is greater than that in a closed channel.

Patterns of wave breaking exhibited large differences over a single tidal cycle. At low tide, wave breaking is more likely to occur on the seaward edge of the channel resulting in a visual classification as a ‘closed’ rip, increasing the likelihood that the rip will form eddies and drifters will be retained in the surfzone. As water level increases towards mid – high tide, the

water depth over the rip head bar is generally too great to induce wave breaking, resulting in a system whereby the rip can be visually classified as 'open'. Under closed conditions, there is also an increase in wave breaking on the adjacent bars in addition to the rip head bar feature, which ultimately reduced the extent of the channel through lateral constriction, whereas the decrease in breaking in open channels lowers wave-current interaction and increases the offshore extent of the rip (Yu and Slinn, 2003). In open channels, the offshore directed current speeds were seen to be 31% lower, consistent with work by Brander and Short (2000), linking lower intensity breaking to lower velocities through morphodynamic scaling.

The observed circulation patterns in this study are consistent with those of Brander (1999) who placed rip dynamics into the context of the Wright and Short (1984) beach state model. They use the underlying morphology over timescales of days to months, whereas this study has discussed the expression of the morphology in terms of patterns of wave dissipation over a single tidal cycle. They describe the transition from longshore bar-trough morphology (LBT), through a rhythmic bar beach (RBB), a transverse bar rip beach (TBR), to a low tide terraced beach (LTT). The LBT-RBB scenario is akin to the open channel described here, with an open connection beyond the surfzone. The feeder channels described for LBT are less obvious or established in the imagery used in the current study, but the gap in the bar is obvious (Figure 8e – f). The TBR/TBR-LTT states are akin to closed channels observed in imagery (Figure 8a – d). The state is characterised by a complete welding of the rip head bar to the adjacent longshore bars. They also note a constriction and increased flow during the transition from LBT [open] towards TBR-LTT [closed]. As progression through the beach states is made, one feeder channel reduces in strength with the opposite channel becoming the dominant feeder for the rip channel. This mirrors observations at Perranporth where the rip channel was predominantly fed from one side (Figure 6c). Austin et al. (2000) discuss similar

transitions as a result of tidal fluctuations, whereby lowering water levels result in the constriction of the channel. Unlike the present study, they show that conditions here described as closed exist without the presence of a rip head bar and suggest that wave-current interactions are an important process at the seaward end of the channel under these conditions.

We have shown here an increase in vorticity through the channel under closed conditions, with vorticity maxima towards the outer edge of the surfzone (Figure 10c). Austin et al. (2014) demonstrated that around low tide, when conditions could be considered closed, that water surface gradients were greatest around the rip neck and over the end of the longshore bars. This difference in water surface gradients (O(0.1 m)) could be a factor controlling the much increased vorticity through the neck of the rip and over bars observed in Figure 10c. Overall, velocities in the closed rips were 31% greater than open channels (Figure 10a, Figure 11a). This is in contrast to the findings of Austin et al. (2014), whereby rip flows were maximised either side of low water. In their study they describe the 'drying' of the feeder and bars, which was not observed here. Therefore, it is likely that the absolute water levels of closed rips in our study and the Austin et al. (2014) conditions of maximum flow were similar. Alongshore-averaged cross-shore velocities are shown to be fairly consistent across the surfzone, with a slight tail off at the offshore extent (Figure 11a). This decreasing velocity was coincident with the location of maximum negative (clockwise) vorticity, potentially explained by wave-current interaction at the offshore extent. Yu and Slinn (2003) demonstrated that in narrower [closed] channels interaction at the offshore extent of the current with the incident wave field was greatest, reducing the strength and extent of currents. This shows agreement with our results that showed a reduction in exits (Figure 9) and current speed at the offshore extent (Figure 11a). The association between increased wave breaking and increased vorticity has been observed before (Houser et al., 2013), where higher intensity

breaking narrowed the available area for the rip channel, which has previously been linked to increased flow speeds (MacMahan et al., 2006). In terms of circulatory patterns, a closed rip here behaves in a similar fashion to the low 'tide factor' rips in the study of Scott et al. (2014), where currents were fed predominantly by one alongshore direction. Here, the current was directed offshore (positive vorticity band in Figure 10c), and as it reached the edge of the surfzone it was again directed alongshore in its original direction (negative vorticity in Figure 10c).

The variation in current speeds and vorticity between open and closed channels may have important implications for sediment transport in the nearshore. Recent research has shown that the dominant driver of sediment suspension and transport in rips is as a result of mean offshore flows (Orzech et al., 2011; Thorpe et al., 2013), with very low frequency (VLF) motions also playing an important role in entrainment and transport of sediment in rips (Aagard and Greenwood, 1995). Our results show increased mean offshore flows under closed channel conditions, and based on these previous studies we can infer that more sediment was suspended under these conditions. However, the vorticity in closed channels was much increased and the dominant circulation pattern was that of surfzone retention. Therefore, under closed conditions, it may be possible that despite the entrainment of greater masses of sediment, the net cross-shore exchange between the surfzone and nearshore is reduced than when compared to open channels. In an open channel, although the flow velocity is reduced (yet not insignificant), the dominant circulatory behaviour is that of surfzone exit, which may be responsible for a greater net offshore mass transport of sediment. This area is certainly worth investigation as part of future studies, as no quantitative measure of sediment transport was made here.

The second objective was to determine how the pattern of wave breaking may influence rip rescue events and hazard to bathers. Exit rates here have been presented under both open or closed conditions and range from 0 – 91 % However, the overall exit rate during the experiment was 36 % which is within the range reported in previous studies elsewhere; 20 % (Castelle et al., 2011, 2013), 46 % (McCarroll et al., 2014b) 0 – 73 % (Scott et al., 2014). In terms of the RNLI data, the results show a greater number, and more serious, incidents occurring when rips were open. After normalising the data, open channels were seen to be twice as dangerous for bathers. Their occurrence, approximately 40 % of the time, accounts for 60 % of the incidents dealt with by the RNLI. Furthermore, they are observed in a disproportionate number of major incidents (78 %) when compared with their overall occurrence over a lifeguard season at Perranporth. The calmer appearance of the surface of rips is cited as a key factor in an inexperienced beach user's decision on where to swim, with the mistaken belief that the seemingly calmer waters away from breaking waves are safer (Sherker et al., 2010; Gallop et al., 2016b). This visual description applies well to the scenario of an open rip channel, where the absence of wave breaking typically extends from the shore to seaward of the surfzone. As a result, casual bathers are more likely to select an open rip channel as a safe area to swim and ultimately increase the risk of ending up in the current. We have shown that the open channel is hydrodynamically more dangerous for bathers and now in addition, the visual signature of an open channel may also increase the likelihood that it is selected by beach users as a place for bathing.

Previous studies have identified high risk activities with regard to rip current related rescues. For example, Woodward et al. (2013) showed that bodyboarders account for 53 % of the rip rescues recorded in the UK. Further investigation of this statistic showed that it can also be linked to the opening and closing of the rip channel. Of the bodyboard incidents investigated here, 73 % occurred under open rip conditions. In an open rip, they are more likely to exit the

surfzone and may therefore become panicked at the distance travelled from the shore, initiating a rescue event. The same applies to swimmers, for whom 88 % of rescue occurred when rip channels were classified as open.

There is currently a paucity of research that effectively links quantitative analysis of video imagery with *in situ* field data with regard to rip research. We have presented here a simple but innovative approach to using video imagery as a first order prediction of rip current hazard. Future work would benefit from the combination of more *in situ* and remotely sensed data, such as particle image velocimetry, to compare breaking patterns with surfzone behaviour. Of particular interest would be investigation into the effect of wave groups on the opening or closing of the rip.

6. Conclusions:

The effect of wave breaking on rip current circulation was investigated using a novel wave breaking parameter defined from video imagery at Perranporth beach, UK. The study was complemented by Lagrangian drifter data that showed closed channel conditions increased the intensity of wave breaking, narrowed the effective channel width and increased both current speed and vorticity in the channel. This promoted surfzone retention and a low exit rate (0 – 24 %). Under open channel conditions, the offshore extent of drifter tracks extended beyond the surfzone under a steady, slower current with much reduced vorticity. The likelihood of surfzone exits increased, with a maximum exit rate during one period reaching 91 %. In the closed channel scenario surfzone retention dominates the nearshore flow regime. However, when the rip channel configuration is open it increases the likelihood of exits, albeit with no guarantee that surfzone exits will be the dominant flow regime. A Chi Squared analysis showed that open channels were statistically more likely to result in rip exits,

compared to closed channels. Furthermore, we hypothesis that the increased flow conditions under closed conditions may entrain more sediment, but the circulatory nature of the flows may ensure that any subsequent transport is more confined to the surfzone than would be the case in open circulations.

The RNLI rip incident database for Perranporth was analysed for trends pertaining to this classification scheme. In open rip scenarios, there were twice as many lives saved and 40 % more rescues overall than compared to closed scenarios. The number of rescues involving open rips was normalised by occurrence, and we conclude that they can be considered twice as dangerous as closed rip channels. At particular risk were bodyboarders who were three times more likely to be rescued from a rip with an open configuration. Also at risk were swimmers, with 88 % of swimmer rescues taking place during 'open' configurations. An open rip configuration would be characterised by less wave breaking and therefore appear calmer and safer for bathing, which may increase the likelihood of their selection as a safe place for bathing. In turn, the flow regime we can now associate with an open rip is notably more dangerous, with the likelihood of surfzone exit increased.

Acknowledgements:

Our thanks go to two anonymous reviewers, as the quality and scope of this manuscript was greatly improved following their constructive review. We thank Tim Scott and Ellie Woodward for their early consultation on research at Perranporth and for their input on drifter design and collection of bathymetric data. Kelvin Aylett of the University of Southampton is thanked for his part in the manufacture, testing and subsequent re-design of the surfzone drifters. We are also grateful to Matthew Wadey, Christos Mitsis, Antony Thorpe, Ellie Woodward, Alex Vincent, Aldous Rees, Kris Inch and Emily Woodhouse for assistance in

the collection of field data. Erwin Bergsma is thanked for assistance with the rectification of Perranporth imagery. Finally, the RNLI are acknowledged for the provision of rip incident data. This research was funded by a 2013 Southampton Marine and Maritime Institute award from the Research Collaboration Stimulus Fund awarded to SG. Additionally, SP received a postgraduate research award from the Royal Geographical Society with the Institute of British Geographers which contributed to field equipment. RR is supported by the AXA Research fund and the Deltares Harbour, Coastal and Offshore engineering Research Programme *'Bouwen aan de Kust*'. The Channel Coastal Observatory and British Oceanographic Data Centre are both acknowledged for the free provision of data.

References:

Aagard, T., Greenwood, B., Nielsen, J., 1997. Mean currents and sediment transport in a rip channel. Marine Geology 140, 24 – 45.

Aagard, T., Greenwood, B., 1995. Longshore and cross-shore suspended sediment transport at far infragravity frequencies in a barred environment. Continental Shelf Research 15, 1235 – 1249.

Austin, M.J., Scott, T.M., Brown, J.A., MacMahan, J.H., 2009. Macrotidal rip current experiment: circulation and dynamics. Journal of Coastal Research SI56, 24 – 28.

Austin, M.J., Scott, T.M., Brown, J., Brown, J.A., MacMahan, J.H., Masselink, G., Russell, P.E., 2010. Temporal observations of rip current circulation on a macro-tidal beach. Continental Shelf Research 30, 1149 – 1165.

Austin, M.J., Scott, T.M., Russell, P.E., Masselink, G., 2013. Rip Current Prediction: Development, Validation, and Evaluation of an Operational Tool. Journal of Coastal Research 29(2), 283 – 300.

Austin, M.J., Masselink, G., Scott, T.M., Russell, P.E., 2014. Water-level controls on macro-tidal rip currents. Continental Shelf Research 75, 28 – 40.

Blossier, B., Bryan, K.R., Daly, C.J., Winter, C., 2016. Nearshore sandbar rotation at single-barred embayed beaches. Journal of Geophysical Research: Oceans, DOI 10.1002/2015JC011031

Bogle, J.A., Bryan, K.R., Black, K.P., Hume, T.M., Healy, T.R., 2001. Video Observations of Rip Formation and Evolution, Journal of Coastal Research SI34, 117 – 127.

Bowen, A.J., 1969. Rip currents: 1. Theoretical investigations. Journal of Geophysical

Research 74, 5467 – 5478.

Brander, R.W., 1999. Field observations on the morphodynamic evolution of a low energy rip current system. Marine Geology 175(3-4), 199 – 217.

Brander, R.W., and Short, A. D., 2000. Morphodynamics of a large-scale rip current system at Muriwai Beach, New Zealand. Marine Geology 165, 27 – 39.

Brander, R.W., and MacMahan, J.H., 2011. Future Challenges for Rip Current Research and Outreach, in: Leatherman, S., Fletemeyer, J. (Eds.), Rip Currents: Beach safety, physical oceanography, and wave modelling. CRC Press, Florida, pp. 1 – 30.

Brighton, B., Sherker, S., Brander, R., Thompson, M., Bradstreet, A., 2013. Rip current related drowning deaths and rescues in Australia 2004-2011. Natural Hazards and Earth Systems 13, 1069-1075. DOI: 10.5194/nhess-13-1069 – 2013.

Castelle, B., Michallet, H., Marieu, V., Bonneton, P., 2011. Surfzone retention in a laboratory rip current. Journal of Coastal Research SI 64, 50 – 54.

Castelle, B., Reniers, A., MacMahan, J., 2013. Numerical modelling of surfzone retention in rip current systems: On the impact of the surfzone sandbar morphology. Proceedings of Coastal Dynamics 2013 (24 – 28 June, Arcachon).

Castelle, B., McCarroll, R.J., Brander, R.W., Scott, T., Dubarbier, B., 2015. Modelling the alongshore variability of optimum rip current escape strategies on a multiple rip-channelled beach. Natural Hazards DOI: 10.1007/s11069-015-2101-3

Cook, D.O., 1970. The occurrence and geologic work of rip currents off Southern California. Marine Geology 9, 173 – 186.

Dalrymple, R.A., 1975. A mechanism for rip current generation on an open coast. Journal of Geophysical Research 80(24), 3485 – 3487.

Gal, Y., Browne, M., Lane, C., 2014. Long-term automated monitoring of nearshore wave height from digital video. IEEE Transactions on Geoscience and Remote Sensing 52(6), 3412 – 3420.

Gallop, S.L., Bryan, K.R., Coco, G., 2009. Video observations of rip currents on an embayed beach, Journal of Coastal Research SI56, 49 – 53.

Gallop, S.L., Bryan, K.R., Coco, G., Stephens, S., 2011. Storm-driven changes in rip channel patterns on an embayed beach. Geomorphology 127, 179 – 188.

Gallop, S.L., Bryan, K.R., Pitman, S.J., Ranasinghe, R., Sandwell, D., 2015. Rip current observations on a low-sloping dissipative beach. Australasian Coasts and Ports Conference, Auckland, New Zealand.

Gallop, S.L., Bryan, K.R., Pitman, S.J., Ranasinghe R., Sandwell, D., 2016a. Pulsations in surf zone currents on a high energy mesotidal beach in New Zealand. Journal of Coastal Research SI75, 912–916.

Gallop, S.L., Woodward, E., Brander, R.W., Pitman, S.J., 2016b. Perceptions of rip current myths from the central south coast of England. Ocean & Coastal Management 119, 14 – 20. DOI: 10.1016/j.ocecoaman.2015.09.010.

Guedes, R.M.C., Calliari, L.J., Holland, K.T., Plant, N.G., Pereira, P.S., 2011. Short-term sandbar variability based on video imagery: Comparison between Time–Average and Time–Variance techniques. Marine Geology 289, 122 – 134.

Hatfield, J., Williamson, A., Sherker, S., Brander, R., Hayen, A., 2012. Development and

evaluation of an intervention to reduce rip current related beach drowning. Accident Analysis and Prevention 46, 45 – 51. DOI: 10.1016/j.aap.2011.10.003

Holman, R.A., Symonds, G., Thornton, E.B., Ranasinghe, R., 2006. Rip spacing and persistence on an embayed beach. Journal of Geophysical Research 111, DOI: 10.1029/2005JC002965.

Holman, R.A., Stanley, J., 2007. The history and technical capabilities of Argus. Coastal Engineering 54, 477 – 491.

Houser, C., Arnott, R., Ulzhöfer, S., Barrett G., 2013. Nearshore circulation over transverse bar and rip morphology with oblique wave forcing. Earth Surface Processes and Landforms 38, 1269 – 1279. DOI: 10.1002/esp.3413

Huntley, D., Saulter, A., Kingston, K., Holman, R., 2009. Use of video imagery to test model predictions of surf heights, in: Brebbia, C.A., Benassai, G., Rodriguez, G.R., (Eds.), Coastal Processes, WIT Transactions on Ecology and the Environment, UK

Kingston, K.S., Ruessink, B.G., Van Eckenvort, I.M.J., Davidson, M.A., 2000. Artificial neural network correction of remotely sensed sandbar location. Marine Geology 169, 137 – 160.

Lippmann, T.C., Holman, R.A., 1989. Quantification of sand bar morphology: a video technique based on wave dissipation. Journal of Geophysical Research 94, 995 – 1011.

Lippmann, T.C., Holman, R.A., 1990. The spatial and temporal variability of sandbar morphology. Journal of Geophysical Research 95, 11575 – 11590.

Longuet-Higgins, M.S., 1970. Longshore currents generated by obliquely incident sea waves: 1. Journal of Geophysical Research 75, 6778 – 6789.

MacMahan, J.H., Thornton, E.B., Reniers, A.J.H.M., 2006. Rip current review. Coastal Engineering 53, 191 – 208.

MacMahan, J.H., Brown, J., Thornton, E., 2009. Low-cost handheld global positioning system for measuring surf-zone currents. Journal of Coastal Research 25(3), 744 – 754.

MacMahan, J., Brown, J., Brown, J.A., Thornton, E., Reniers, A., Stanton, T., Henriquez, M., Gallagher, E., Morrison, J., Austin, M.J., Scott, T.M., Senechal, N., 2010. Mean Lagrangian flow behavior on an open coast rip-channelled beach: A new perspective. Marine Geology 268, 1 – 15.

Masselink, G., Austin, M.J., Scott, T., Russell, P., 2014. Role of wave forcing, storms and NAO in outer bar dynamics on a high-energy, macro-tidal beach. Geomorphology 226, 76 - 93. DOI: 10.1016/j.geomorph.2014.07.025

McCarroll, R.J., Brander, R.W., MacMahan, J.H., Turner, I.L., Reniers, A.J.H.M., Brown, J.A., Bradstreet, A., Sherker, S., 2014a. Evaluation of swimmer-based rip current escape strategies. Natural Hazards 71, 1821 – 1846.

McCarroll, R.J., Brander, R.W., Turner, I.L., Power, H.E., Mortlock, T.R., 2014b. Lagrangian observations of circulation on an embayed beach with headland rip currents. Marine Geology 355, 173 – 188.

McCarroll, R.J., Castelle, B., Brander, R.W., Scott, T., 2015. Modelling rip current flow and bather escape strategies across a transverse bar and rip channel morphology. Geomorphology 246, 502 – 518.

Miloshis, M., Stephenson, W.J., 2011. Rip current escape strategies: lessons for swimmers and coastal rescue authorities. Natural Hazards 59, 823 – 832.

Molinari, R., Kirwan, A.D., 1975. Calculations of differential kinematic properties from Lagrangian observations in the Western Caribbean Sea. Journal of Physical Oceanography 5: 483 – 491.

Orzech, M.D., Reniers, A.J.H.M., Thornton, E.B., MacMahan, J.H., 2011. Megacusps on rip channel bathymetry: Observations and modelling. Coastal Engineering 58, 890 – 907.

Pitman, S.J., Gallop, S.L., Haigh, I.D., Mahmoodi, S., Masselink, G., Ranasinghe, R., 2016. Synthetic imagery for the automated detection of rip currents. Journal of Coastal Research SI75, 912 – 916.

Plant, N.G., Holman, R.A., 1998. Extracting morphologic information from field data. Proceedings of the 26th International Coastal Engineering Conference, ASCE, New York, USA, pp. 2773 – 2784.

Quartel, S., 2009. Temporal and spatial behaviour of rip channels in a multiple-barred coastal system. Earth Surfaces Processes and Landforms 34, 163-176. DOI: 10.1002/esp.1685

Ranasinghe, R., Symonds, G., Holman, R., 1999. Quantitative characterisation of rip dynamics via video imaging, in: Kraus, N.C., McDougal, W.G., (Eds.), Coastal Sediments '99, American Society of Civil Engineers, Reston, USA, pp. 987 – 1002.

Ranasinghe, R., Symonds, G., Black, K., Holman, R. 2004. Morphodynamics of intermediate beaches: a video imaging and numerical study. Coastal Engineering 51, 629 – 655. DOI: 10.1016/j.coastaleng.2004.07.018

Schmidt, W.E., Woodward, B.T., Millikan, K.S., Guza, R.T., Raubenheimer, B., Elgar, S., 2003. A GPS-tracked surf zone drifter. Journal of Atmospheric and Oceanic Technology 20, 1069 – 1075.

Scott, T.M., Russell, P.E., Masselink, G., Wooler, A., 2008. High volume sediment transport and its implications for recreational beach risk. Proceedings of the 31st International Conference on Coastal Engineering, Hamburg, pp. 4250 – 4262.

Scott, T.M., Masselink, G., Austin, M.J., Russell, P.E., 2014. Controls on macrotidal rip current circulation. Geomorphology 214, 198 – 215.

Scott, T.M., Austin, M., Masselink, G., Russell, P., 2016. Dynamics of rip currents assosciated with groynes – field measurements, modelling and implications for beach safety. Coastal Engineering 107, 53 – 69.

Shepard, F.P., Emery, K.O., La Fond, E.C., 1941. Rip currents: A process of geological importance. The Journal of Geology 49(4), 337 – 369.

Sherker, S., Williamson, A., Hatfield, J., Brander, R., Hayen, A., 2010. Beachgoers' beliefs and behaviours in relation to beach flags and rip currents. Accident Analysis & Prevention 42, 1785 – 1804. DOI: 10.1016/j.aap.2010.04.020

Sonu, C.J., 1972. Field observation of nearshore circulation and meandering currents. Journal of Geophysical Research 77(18), 3232 – 3247.

Spydell, M., Feddersen, F., Guza, R.T., 2007. Observing surf-zone dispersion with drifters. Journal of Physical Oceanography 37, 2920 – 2939.

Thorpe, A., Miles, J., Masselink, G., Russell, P., Scott, T., Austin, M., 2013. Suspended sediment transport in rip currents on a macrotidal beach. Journal of Coastal Research SI65, 1880 – 1885.

Turner, I.L., Whyte, D., Ruessink, B.G., Ranasinghe, R., 2007. Observations of rip spacing, persistence and mobility at a long, straight coastline. Marine Geology 236, 209 – 221.

Van Leeuwen, B.R., McCarroll, R.J., Brander, R.W., Turner, I.L., Power, H.E., Bradstreet, A.J., 2015. Examining rip current escape strategies in non-traditional beach morphologies. Natural Hazards DOI: 10.1007/s11069-015-2072-4

Whyte, D., Turner, I.L., Ranasinghe, R., 2005. Rip Characterisation on the Gold Coast, Australia: An Analysis using Coastal Imaging Techniques, in: Coasts and Ports 2005: Coastal Living - Living Coast. Adelaide, Australia.

Woodward, E., Beaumont, E., Russell, P., Wooler, A., Macleod, R., 2013. Analysis of rip current incidents and victim demographics in the UK. Journal of Coastal Research SI65, 850 – 855.

Wright, L.D., Chappell, J., Thom, B.G., Bradshaw, M.P., Cowell, P., 1979. Morphodynamics of reflective and dissipative beach and inshore systems: Southeastern Australia. Marine Geology 32, 105 – 140.

Wright, L.D., Short, A.D., 1984. Morphodynamic variability of surf zones and beaches: A synthesis. Marine Geology 56, 93 – 118. DOI: 10.1016/0025-3227(84)90008-2

Yu, J., Slinn, D.N., 2003. Effects of wave-current interaction on rip currents. Journal of Geophysical Research 108(C3), 3088. DOI: 10.1029/2001JC001105

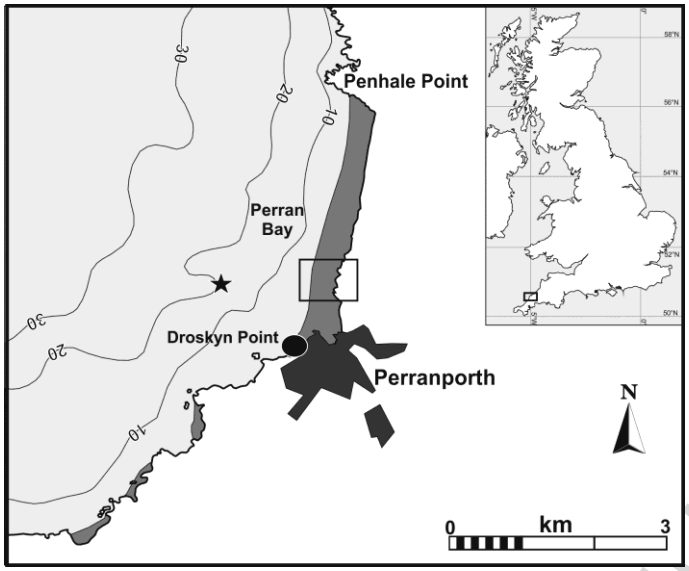

Figure 1

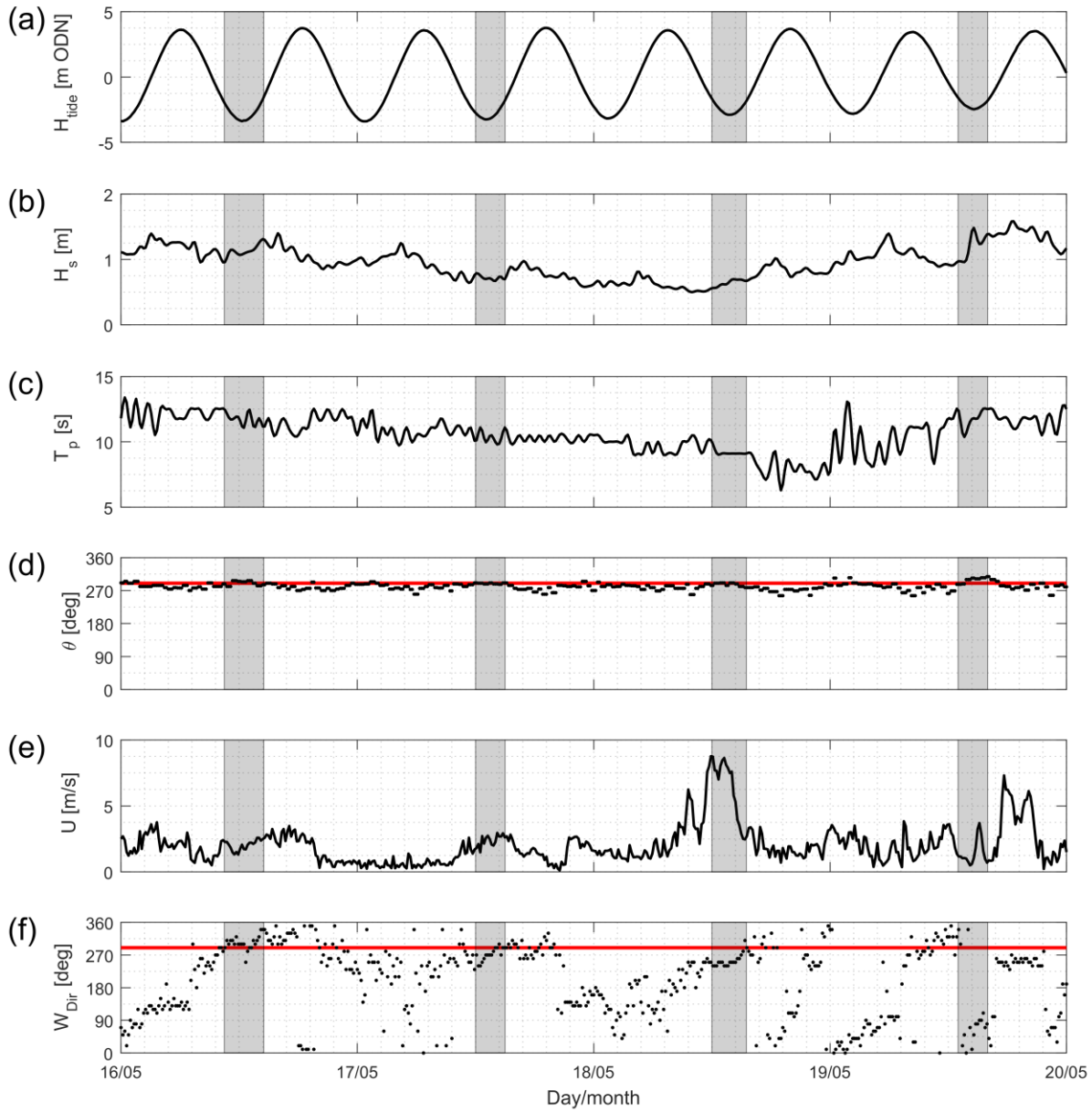

Figure 2

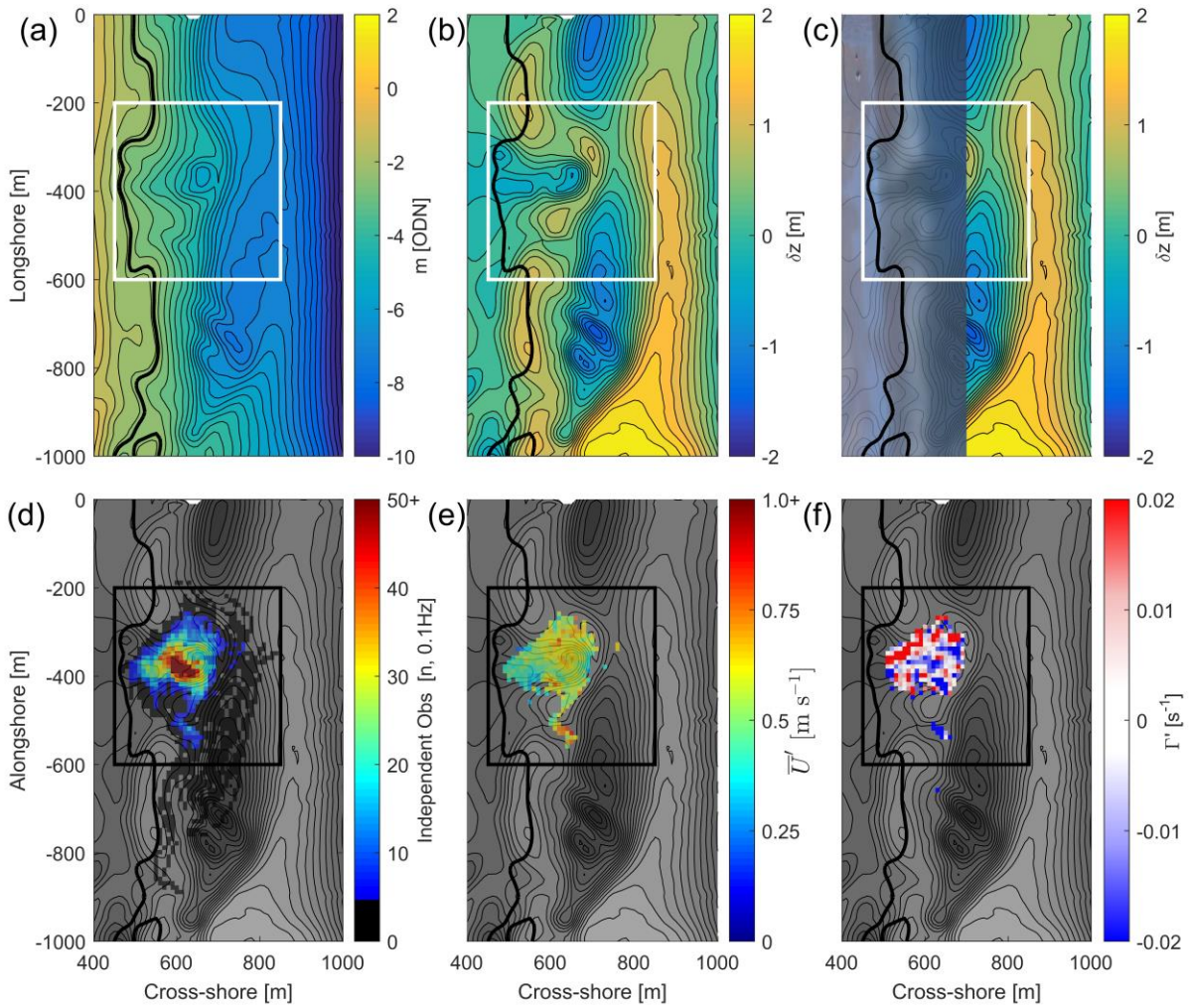

Figure 3

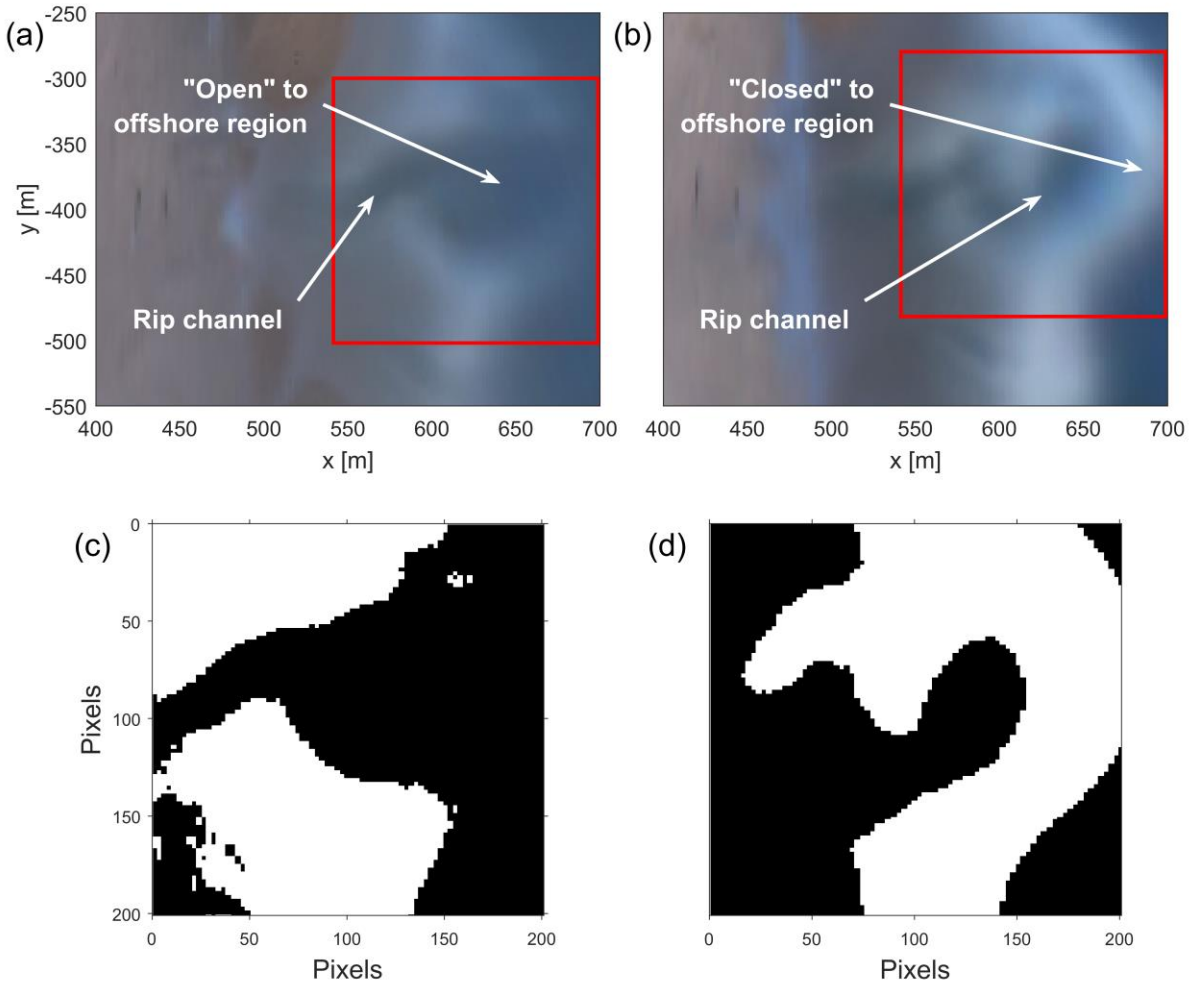

Figure 4

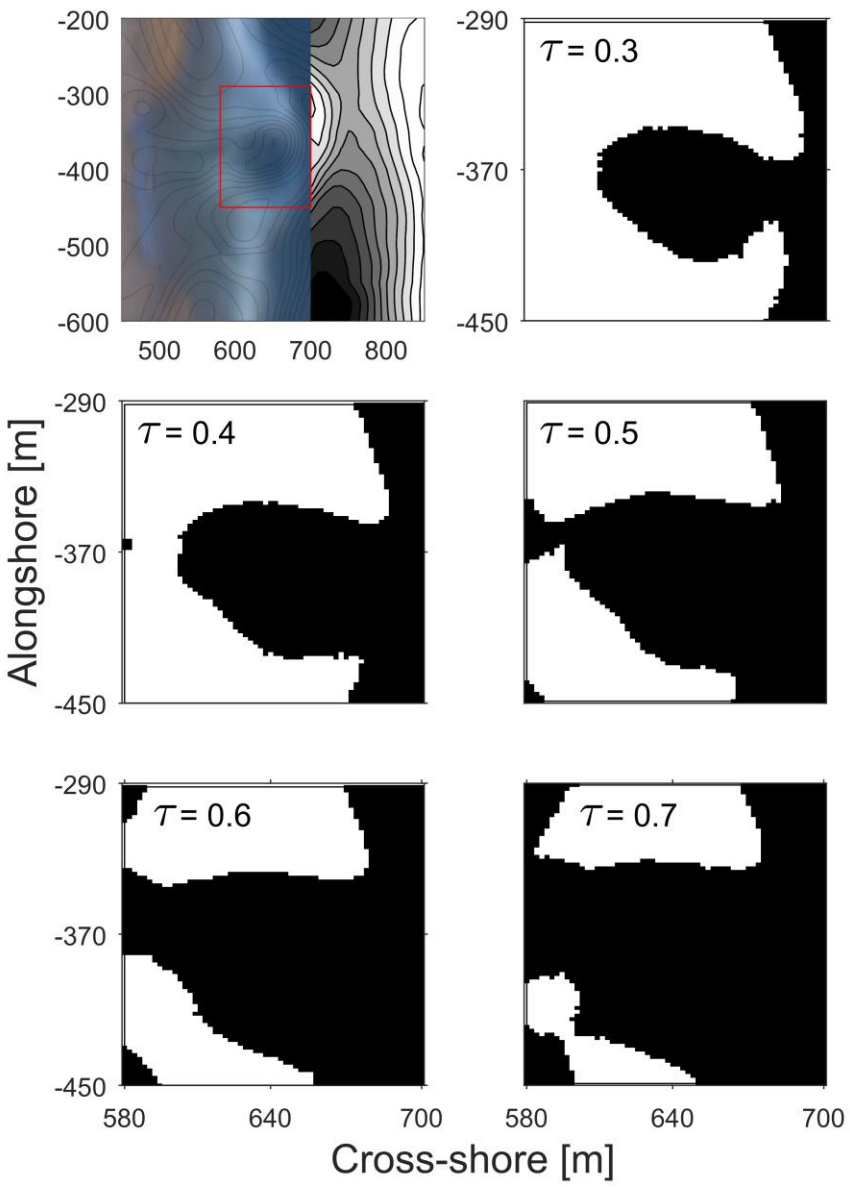

Figure 5

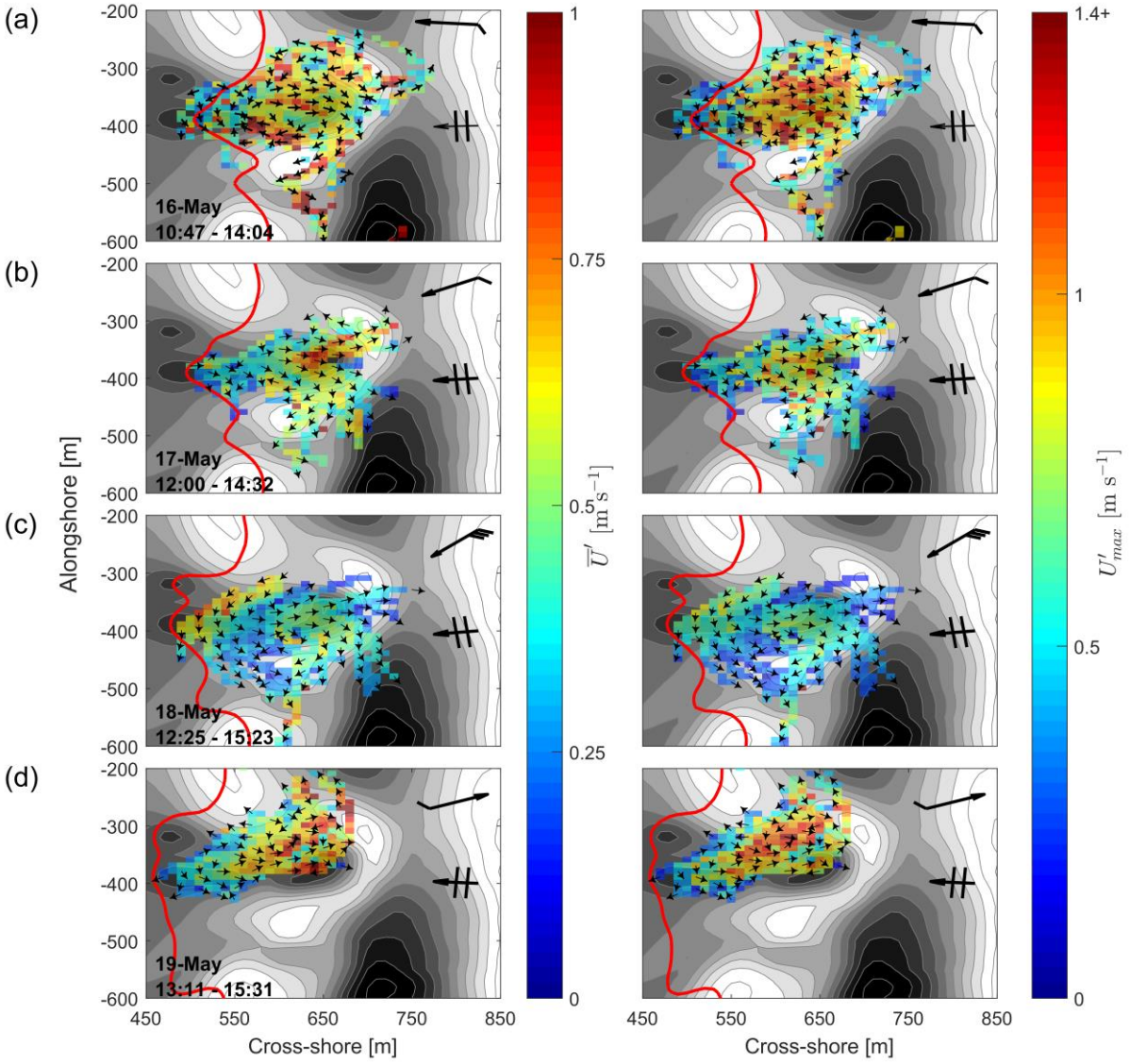

Figure 6

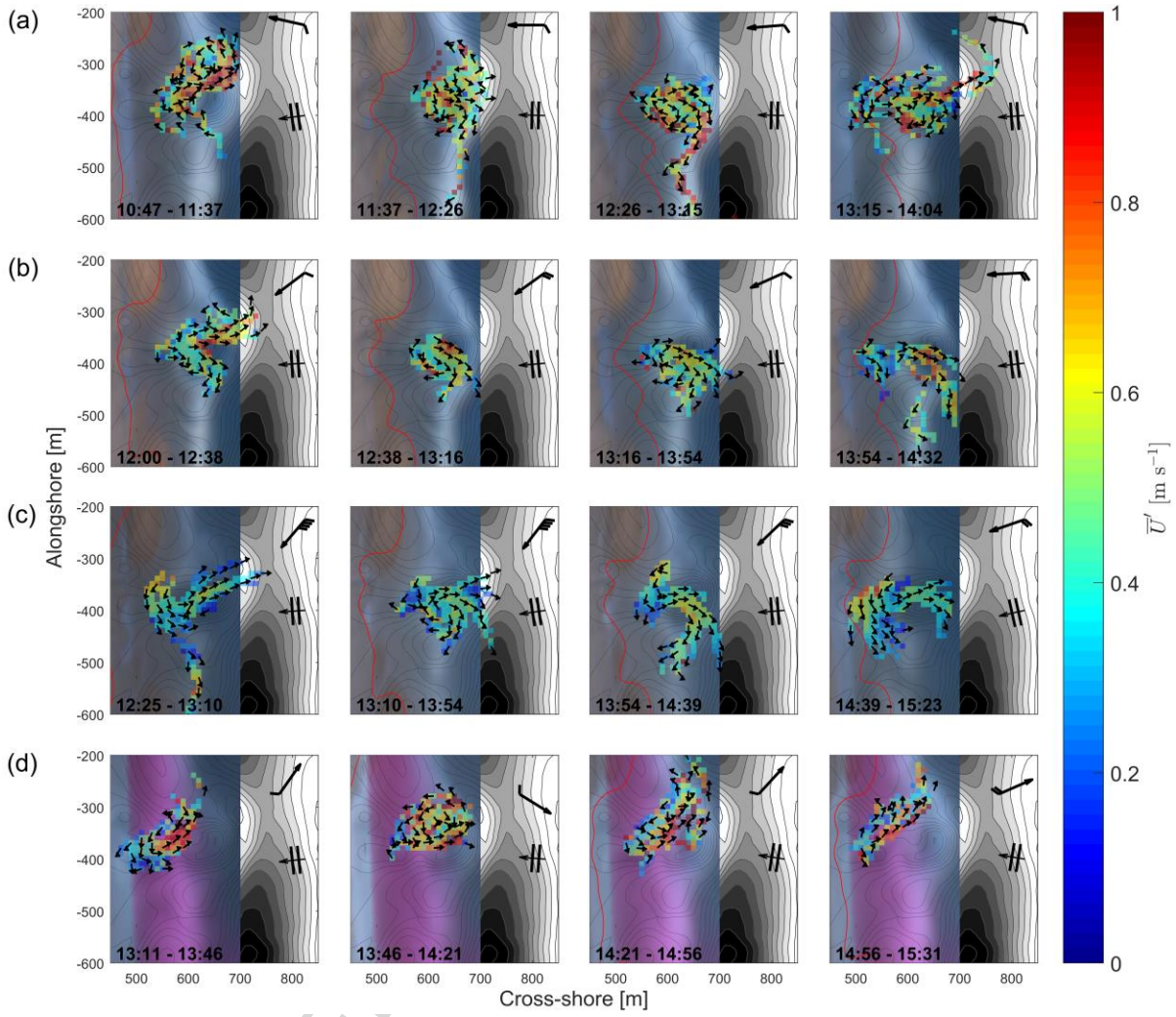

Figure 7

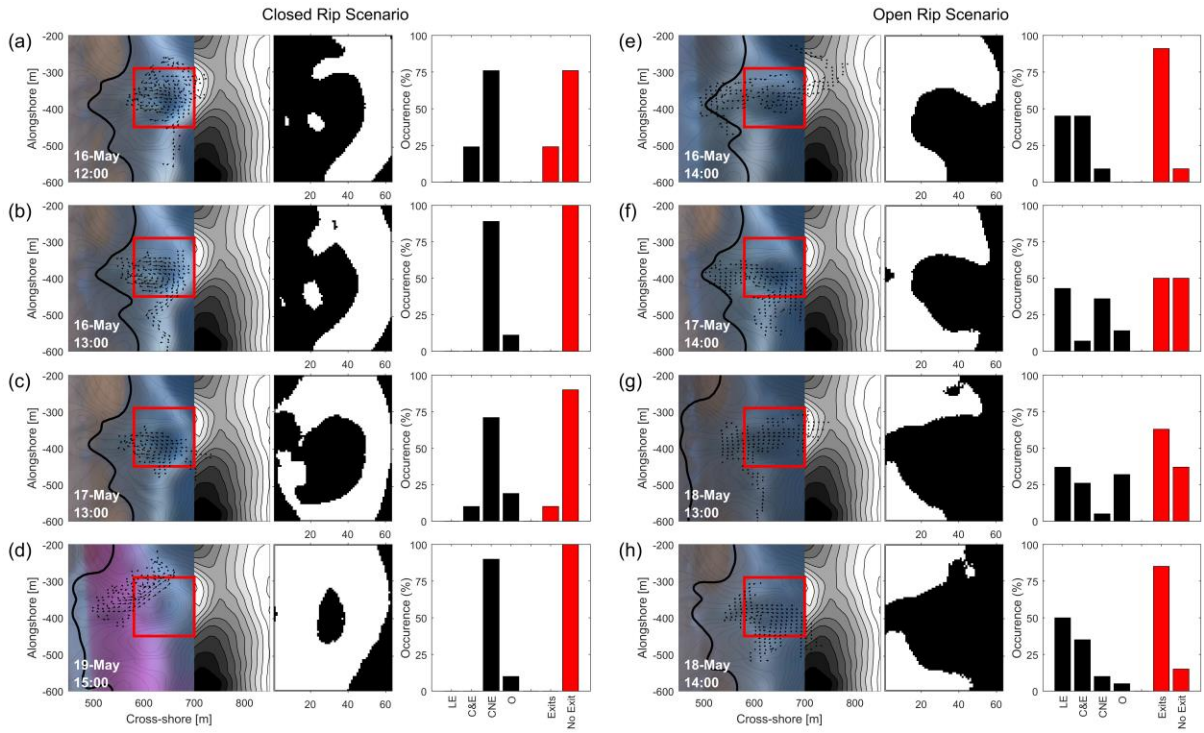

Figure 8

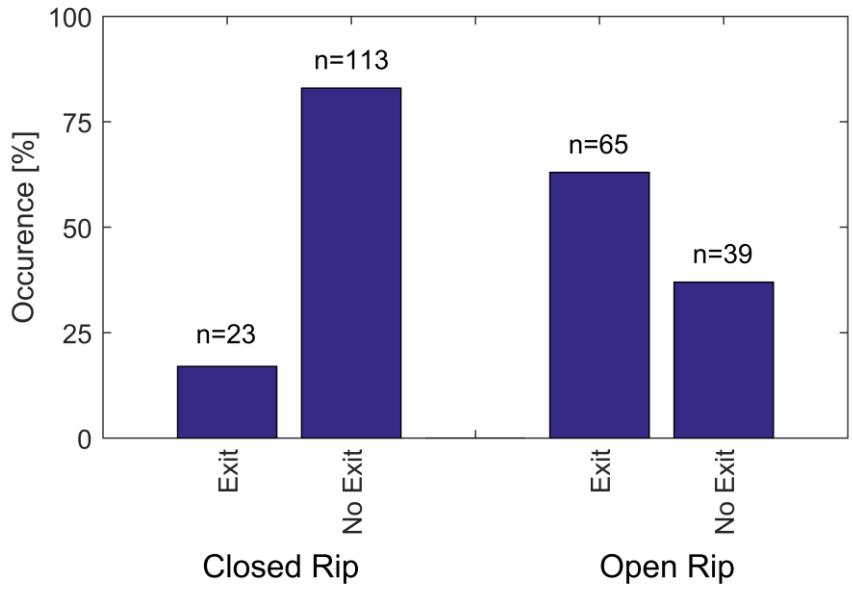

Figure 9

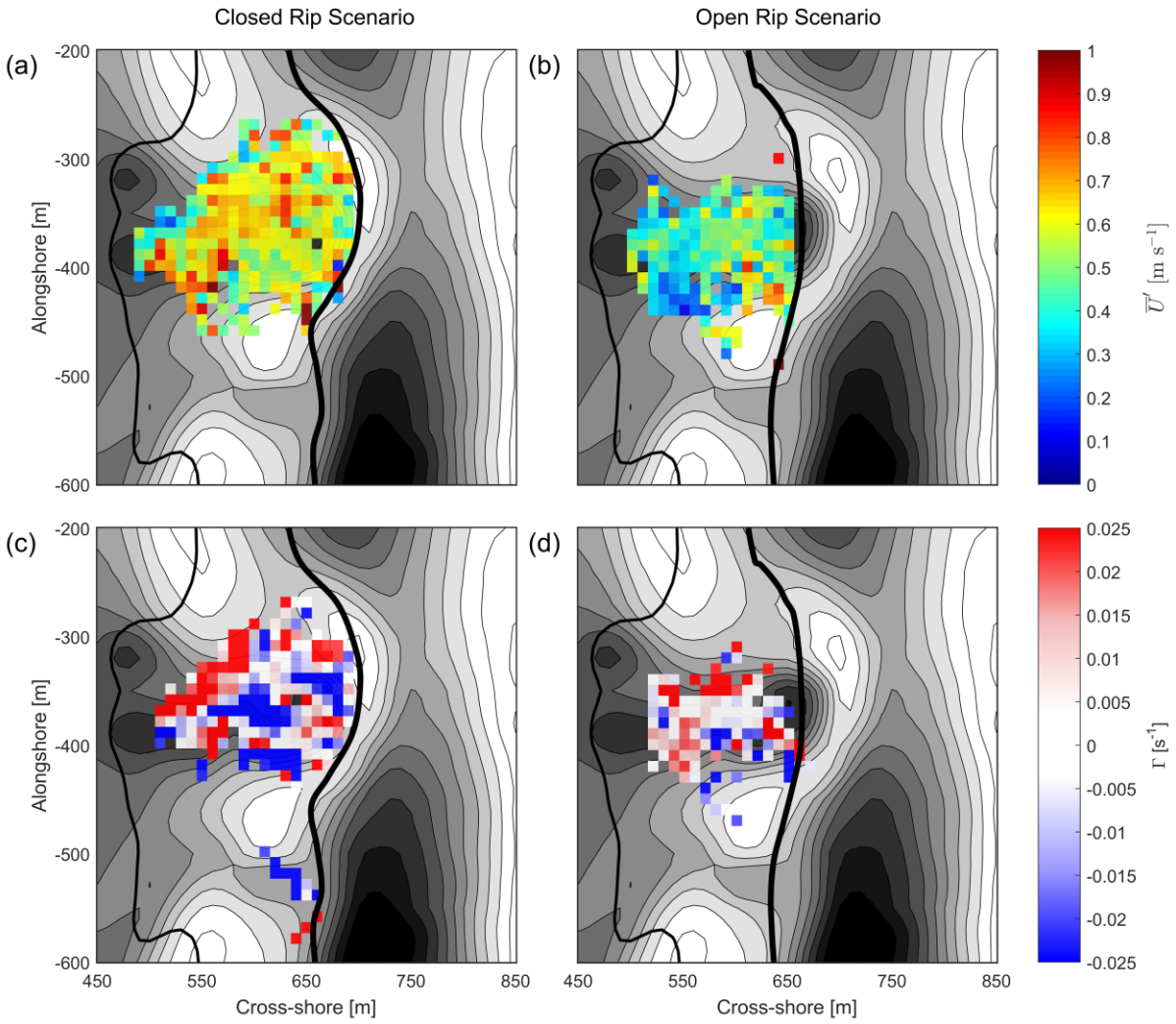

Figure 10

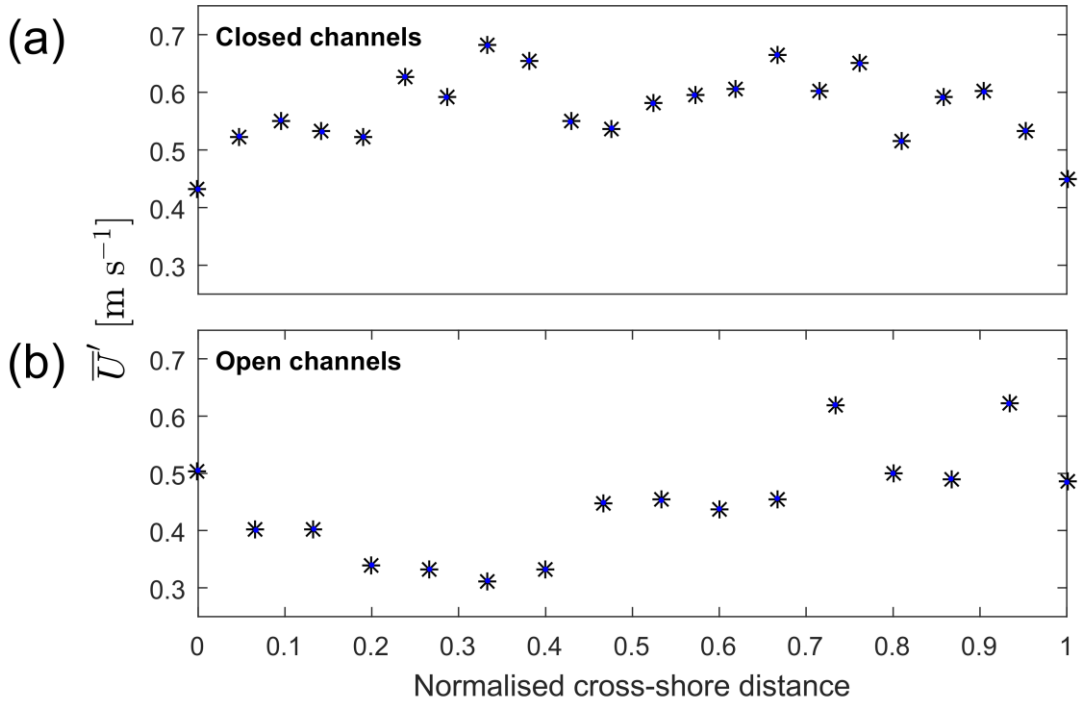

Figure 11

Figure 1. Map of Perranporth with the field study location enclosed by a black box. The black circle shows the position of the Argus camera station, and the star the directional Waverider wave buoy.

Figure 2. Summary of field conditions from 16 to 20 May 2014 at Perranporth beach, with vertical grey bars indicating drifter deployments: a) water level H_{tide}; b) significant wave height H_s; c) peak wave period T_p; d) incident wave direction θ; e) wind speed U; and f) wind direction W_{Dir}. Red lines indicate the shore-normal direction. ODN refers to Ordnance Datum Newlyn, which is approximate Mean Sea Level in the UK.

Figure 3. Bathymetry and drifter data for the field experiment with white boxes indicative of study area and solid black line is 0 m ODN. (a) The merged bathymetric and topographic data, measured on 17 May 2014. (b) The residual morphology. (c) The overlay of merged, rectified images from the Argus camera onto the bathymetry. (d) Number of independent observations recorded at 0.1 Hz over the study period, binned into 10 x 10 m grid squares. Grid squares with less than 5 observations appear as grey and are not considered further in the paper. (e) Maximum drifter velocities recorded during the experiment. (f) Overall surfzone vorticity over the experiment, with red values indicative of an anti-clockwise horizontal rotation, and blue values indicative of clockwise rotation.

Figure 4. Examples of rip currents from Perranporth beach, U.K. The examples here are classified as (a) 'open'; and (b) 'closed' to the offshore region, by wave breaking. The classification is achieved through thresholding. (c) Open channels extend as black pixels from the extreme left of the area and have an open connection to the offshore area. (d) Closed channels are segregated from the offshore region by a distinct band of white pixels, indicative of wave breaking.

Figure 5. Sensitivity analysis for the application of the Pitman et al., (2016) method. An original, rectified, timex image from Perranporth (top left) with area of the surfzone incorporating a rip channel used for thresholding (red box). Thresholds (τ) from 0.3 – 0.7 were tested, and in all the cases shown in the figure, the rip current was classified as 'open', irrespective of the selected threshold within that range.

Figure 6. Daily observations from drifter deployments. Mean (left column) and maximum (right column) observed velocity is presented as the underlying colour on grid with cells of 10 x 10 m for the (a) 16th, (b) 17th, (c) 18th, and (d) 19th May 2014 deployments. The overlaid arrows indicate the dominant direction of flow in each grid square. Wind direction is indicated in the top right, with each barb indicating increments of 2.5 m s^{-1} in the average wind speed. Dominant direction of wave propagation is given by the symbol at mid height on the right hand side of each panel, and the lowest still water elevation for each day is given as a solid red line.

Figure 7. Drifter observations binned into approximately 45 minute periods throughout the experiment, with (a) 16 May, (b) 17 May, (c) 18 May, and (d) 19 May presented on individual rows. Timing of the observations is given in each panel. Mean observed velocity is presented as the underlying colour on grid with cells of 10 x 10 m. The overlaid arrows

indicate the dominant direction of flow in each grid square. Wind direction is indicated in the top right, with each barb indicating increments of 2.5 m s^{-1} in the average wind speed. Dominant direction of wave propagation is given by the symbol at mid height on the right hand side of each panel, and the lowest still water elevation for each period is given as a solid red line.

Figure 8. Rip current flow regimes under open and closed channel conditions. (a – d) Closed and (e – h) open channel scenarios observed during the field experiment. The left hand panel shows the drifter plots for that individual hour of observation, binned into a 10 x 10 m grid, with black arrows indicative of flow direction, with a solid black line indicative of the lowest still water elevation during that period. The red box indicates the part of the channel the classification algorithm was applied to, with the results presented in the middle panel. Black pixels are indicative of both channels and the offshore area, with white pixels representative of wave breaking. The various behaviours observed (right panel) are presented, with each drift classified as either a linear exit (LE), circulation followed by an exit (C&E), circulation with no exit (CNE), or 'other' (O). The right hand two bars represent overall behaviour, with 'Exit' constituting the sum of LE and C&E behaviours, and 'No Exit' the product of CNE and O behaviours.

Figure 9. A summary of all behaviours observed during the 4-day field campaign, split into (left) closed and (right) open scenarios. Exits were defined as the sum of 'Linear exit' and 'Circulation then exit' scenarios, whereas the No Exit total was the sum of 'Circulation, no exit' and 'Other' scenarios. In total, there are 240 individual drifts classified.

Figure 10. Offshore-directed current speeds (top) and vorticities (bottom), derived from surfzone measurements in closed (left) and open (right) rip channels. The thin black line is indicative of the mean shoreline position during deployments, with the thick black line indicative of typical surfzone limits in closed (a and c) and open (b and d) rip channels. In the vorticity plots, positive/red values show an anticlockwise horizontal rotation in the fluid, whereas negative/blue is indicative of clockwise rotation.

Figure 11. Alongshore-averaged, cross-shore velocity profiles for closed (top) and open (bottom) rips. All alongshore observations have been accounted for at each cross-shore location. The cross-shore location is normalized between minimum and maximum extents of the surfzone in closed and open channels respectively. Normalisation was necessary as typically, the surfzone under open conditions was approximately 25% narrower.

Table 1. Analysis of rip incident data for Perranporth beach between 2009 – 2013. For each reported incident, the contemporaneous image has been located and the rip channel classified as open or closed. Below is a summary of the type of incident, and the narrative of confounding factors recorded by the lifeguard.

Table 1

	Type of incident			Involving		
Channel classification	Life saved	Rescue	Assistance	Body boarder	Swimmer	Inexperience
Open	10	169	81	97	18	35
Closed	3	122	104	30	2	16

Highlights

- A novel wave breaking parameter for investigation of rip currents
- Rips classified as open or closed in terms of wave breaking at rip head
- Wave breaking patterns shown to be a key driver of surfzone exit rate
- Open rips shown to be twice as dangerous as closed rips